Formation of Palladium(0) Complexes from $Pd(OAc)_2$ and a Bidentate Phosphine Ligand (dppp) and Their Reactivity in Oxidative Addition

Christian Amatore,* Anny Jutand,* and Audrey Thuilliez

Département de Chimie, Ecole Normale Supérieure, UMR CNRS 864024, Rue Lhomond, F-75231 Paris Cedex 5, France

Received February 12, 2001

A Pd^0 complex is spontaneously generated from $Pd(OAc)_2$ and a bidentate phosphine such as dppp (1,3-bis(diphenylphosphino)propane). dppp is the reducing agent and is oxidized to the hemioxide dppp(O). The intramolecular reduction step is reversible. A stable Pd^0 complex is quantitatively formed in the presence of 2 equiv of dppp, water, and a base (NEt_3). The oxidative addition of PhI gives a cationic complex, $PhPd(dppp)(dppp(O))^+$, in which dppp(O) behaves as a monodentate ligand. $PhPd(OAc)(dppp)$ is formed in the presence of added AcO^-. The oxidative addition of PhI is an intricate reaction whose kinetics has been investigated only in the presence of added AcO^-. It involves reactive dimeric or/and monomeric Pd^0 complexes ligated by AcO^- whose relative reactivity is a function of the PhI concentration.

Introduction

It has been established that a Pd^0 complex is spontaneously formed from $Pd(OAc)_2$ and monodentate phosphine ligands by an irreversible intramolecular reduction of a Pd^{II} complex by the phosphine (Scheme 1).[1] Phosphine oxide is formed in the reduction process.

Scheme 1. Mechanism of the Formation of Pd^0 from $Pd(OAc)_2$ and PPh_3

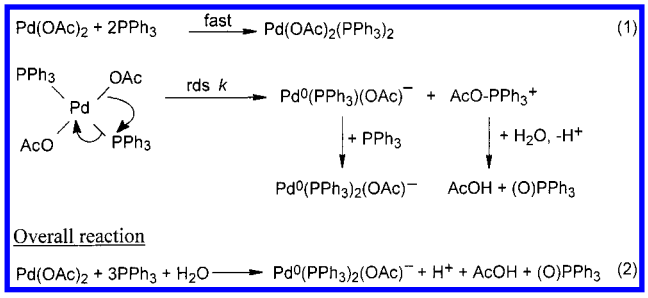

At least 3 equiv of PPh_3 are required to get a stable anionic 16-electron complex, $Pd^0(PPh_3)_2(OAc)^-$ (eq 2), in which one acetate of the $Pd(OAc)_2$ precursor remains ligated to the Pd^0 center.[2] $Pd^0(PPh_3)_2(OAc)^-$ is the reactive species in oxidative addition of phenyl iodide (eq 3), which yields the unexpected $PhPd(OAc)(PPh_3)_2$ complex.[1,2] The latter is the reactive species in Heck reactions, establishing the important role played by the acetate ions delivered by the catalytic precursor (Scheme 2).[2,3]

$$Pd^0(PPh_3)_2(OAc)^- + PhI \longrightarrow PhPd(OAc)(PPh_3)_2 + I^- \quad (3)$$

Addition of bidentate bisphosphine ligands to $Pd(OAc)_2$ also provides efficient catalytic precursors for many Pd-catalyzed reactions,[4−7] among them the Heck reactions.[5−7] Chiral bisphosphine ligands may induce asymmetric reactions.[6] The spontaneous formation of

Scheme 2. Mechanism of the Heck Reaction Performed with the Catalytic Precursor: $Pd(OAc)_2$ and PPh_3

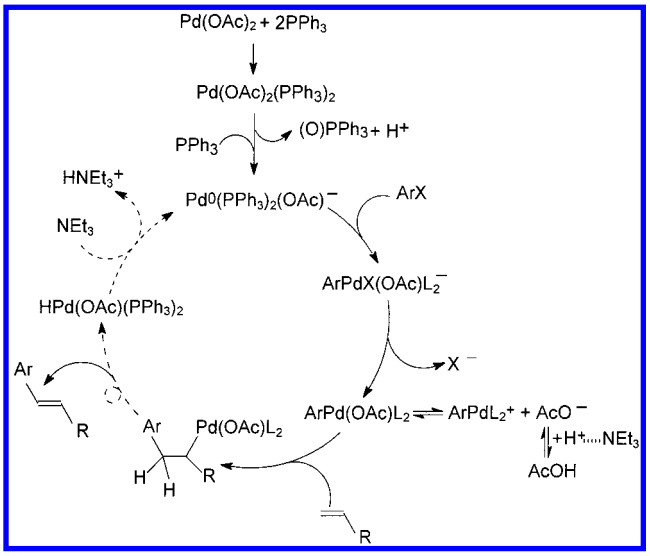

[a] The steps that have been fully characterized kinetically are indicated using solid arrows, while the others are shown with dashed arrows.[3]

* Correponding authors. Fax: 33 1 44 32 33 25. E-mail: Anny.Jutand@ens.fr and amatore@ens.fr.

(1) (a) Amatore, C.; Jutand, A.; M'Barki, M. A. *Organometallics* **1992**, *11*, 3009. (b) Amatore, C.; Carré, E.; Jutand, A.; M'Barki, M. A. *Organometallics* **1995**, *14*, 1818.
(2) Amatore, C.; Carré, E.; Jutand, A.; M'Barki, M. A.; Meyer, G. *Organometallics* **1995**, *14*, 5605.
(3) Amatore, C.; Jutand, A. *Acc. Chem. Res.* **2000**, *33*, 314.
(4) Tsuji, J. *Organic Synthesis via Palladium Compounds*; Springer-Verlag, New York, 1980.
(5) (a) de Mejeire, A.; Meyer, F. E. *Angew. Chem., Int. Ed. Engl.* **1994**, *33*, 2379. (b) Kondo, K.; Sodeoka, M.; Mori, M.; Shibasaki, M. *Synthesis* **1993**, 920. (c) Cabri, W.; Candiani, I. *Acc. Chem. Res.* **1995**, *28*, 2.

10.1021/om0101137 CCC: $20.00
Publication on Web 06/21/2001

a Pd^0 complex, $Pd^0(Binap)_2$, from $Pd(OAc)_2$ associated with 3 equiv of Binap (2,2′-bis(diphenylphosphino)-1,1′-binaphthyl) has been reported by Hayashi and Osawa.[8] Binap has been identified as the chemical reducer, which is oxidized to the hemioxide Binap(O). In this case, the formation of the Pd^0 complex is significantly accelerated by addition of water.

We report here mechanistic investigations on the mechanism of formation of Pd^0 complexes from $Pd(OAc)_2$ and *n* equiv ($n = 1-3$) of dppp (1,3-bis(diphenylphosphino)propane, $PPh_2(CH_2)_3PPh_2$)[7] as a prototype of chelating bisphosphines and on their reactivity in oxidative addition. In contrast to PPh_3, which is oxidized to $(O)PPh_3$ (Scheme 1), an insignificant poor ligand that does not play any role in catalytic reactions, the situation is expected to be much more complicated in the case of bidentate ligands. Indeed, the mono-oxidation of $PPh_2(CH_2)_3PPh_2$ provides a hemioxide ligand, PPh_2-$(CH_2)_3PPh_2(O)$ (named dppp(O) in the following), which still remains a monodentate phosphine ligand able to coordinate palladium complexes.

Results and Discussion

Evidence for the Formation of Palladium(0) Complexes from $Pd(OAc)_2$ and dppp in DMF. $Pd(OAc)_2$ + 1 equiv of dppp. Addition of 1 equiv of dppp to $Pd(OAc)_2$ in DMF (containing nBu_4NBF_4, 0.3 M) results in the formation of a yellow-orange solution, which exhibited a reduction peak at $E^p = -1.47$ V vs SCE.[9] The complex formed in solution was relatively stable at room temperature, as attested by its constant reduction peak current intensity (the current intensity is proportional to the electroactive species concentration). The complex exhibited a broad ^{31}P NMR singlet at 11.0 ppm ($\Delta\nu_{1/2} = 30$ Hz), which was assigned to $Pd(OAc)_2(dppp)$ (eq 4).[10] No oxidation peak was detected when the cyclic voltammetry was performed directly in oxidation, suggesting that either no Pd^0 complex was spontaneously formed from $Pd(OAc)_2(dppp)$ or that a Pd^0 complex is formed but via a slow and endergonic equilibrium (eq 5 in Scheme 3), at a very low concentration, preventing any detection by cyclic voltammetry or ^{31}P NMR spectroscopy.

The equilibrium (eq 5) could be shifted toward its right-hand side, either by water addition[11] (Scheme 3)

Scheme 3. Tentative Mechanism for the Formation of Pd^0 from $Pd(OAc)_2$ and 1 equiv of dppp

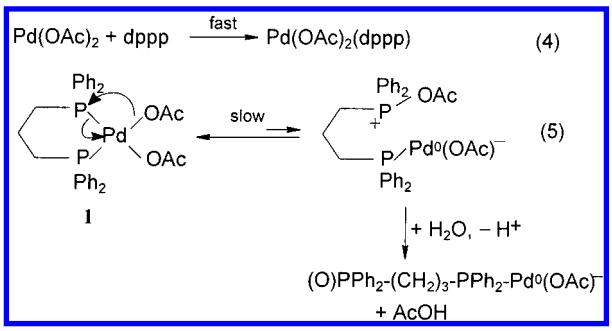

or by reaction of PhI in an oxidative addition. Addition of water in large excess did not induce any formation of a Pd^0 complex, which could have been detected in cyclic voltammetry. The ^{31}P NMR singlet of $Pd(OAc)_2$-(dppp) was not affected by the presence of water or PhI added in excess (10 equiv). No new signal appeared, which could have characterized a (phenyl)palladium(II) complex formed by oxidative addition of PhI to a Pd^0 complex. The formation of a Pd^0 complex is then thermodynamically not favored.

At higher temperature (48 °C), the solution progressively turned to dark brown with formation of black palladium, which could not be characterized either by cyclic voltammetry or by ^{31}P NMR. The reduction peak of $Pd(OAc)_2(dppp)$ progressively disappeared, suggesting that a Pd^0 complex was progressively formed but was too unstable[12] because of a lack of coordinating ligand, excluding thus any fine kinetic investigation.

$Pd(OAc)_2$ + 2 equiv of dppp. The situation changed dramatically when 2 equiv of dppp was added to $Pd(OAc)_2$ (2 mM) in DMF. Indeed, at room temperature, the reduction peak current intensity of $Pd(OAc)_2(dppp)$ at $E^p = -1.51$ V vs SCE (R_1 in Figure 1a) decreased with time, while an oxidation peak O_1 at $E^p = -0.41$ V was observed (Figure 1b) whose oxidation peak current intensity increased as a function of time. This oxidation peak disappeared in the presence of PhI; consequently it characterizes a Pd^0 complex. The formation of the Pd^0 complex was also monitored by ^{31}P NMR spectroscopy. The magnitude of the signal of $Pd(OAc)_2(dppp)$ at 11.0 ppm decreased with time, while a new singlet was detected at 4.20 ppm and assigned to a Pd^0 complex, which disappeared in the presence of PhI. Two other signals were also detected at 29.6 and −17.0 ppm and assigned to the hemioxide $PPh_2(CH_2)_3PPh_2(O)$ by comparison with an authentic sample of dppp after oxidation by dioxygen. The former signal characterizes the phosphine oxide $O{=}PPh_2-$, the latter the phosphine $-PPh_2$ of dppp(O).

This establishes that (i) a stable Pd^0 complex is formed at room temperature from $Pd(OAc)_2(dppp)$, in the presence of 2 equiv of dppp per $Pd(OAc)_2$, and (ii) dppp is the reducing agent. The ^{31}P NMR singlet of $Pd(OAc)_2(dppp)$ disappeared completely only after ad-

(6) (a) Osawa, F.; Kubo, A.; Hayashi, T. *J. Am. Chem. Soc.* **1991**, *113*, 1417. (b) Hayashi, T.; Kubo, A.; Ozawa, F. *Pure Appl. Chem.* **1992**, *64*, 421. (c) Ozawa, F.; Kubo, A.; Matsumoto, Y.; Hayashi, T.; Nishioka, E.; Yanagi, K.; Moriguchi, K. *Organometallics* **1993**, *12*, 4188. (d) Shimizu, I.; Matsumoto, Y.; Shoji, K.; Ono, T.; Satake, A.; Yamamoto, A. *Tetrahedron Lett.* **1996**, *37*, 7115. (e) Shibasaki, M.; Boden, C. D. J.; Kojima, A. *Tetrahedron* **1997**, *53*, 7371. (f) Shibasaki, M.; Vogl, E. M. *J. Organomet. Chem.* **1999**, *576*, 1.

(7) For Heck reactions catalyzed by $Pd(OAc)_2$ and dppp, see ref 5c and: (a) Cabri, W.; Candiani, I.; DeBernardinis, S.; Francalanci, F.; Penco, S.; Santi, R. *J. Org. Chem.* **1991**, *56*, 5796. (b) Cabri, W.; Candiani, I.; Bedeshi, A.; Penco, S.; Santi, R. *J. Org. Chem.* **1992**, *57*, 1481. (c) Cabri, W.; Candiani, I.; Bedeshi, A.; Santi, R. *J. Org. Chem.* **1992**, *57*, 3358. (d) Herrmann, W. A.; Broβmer, C.; Öfele, K.; Beller, M.; Fisher, H. *J. Mol. Catal. A* **1995**, *103*, 133. (e) Larhed, M.; Hallberg, A. *J. Org. Chem.* **1996**, *61*, 9582. (f) Vallin, K. S. A.; Larhed, M.; Johansson, K.; Hallberg, A. *J. Org. Chem.* **2000**, *65*, 4537. (g) Qadir M.; Möchel, T.; Hii, K. K. *Tetrahedron* **2000**, *56*, 7975.

(8) Ozawa, F.; Kubo, A.; Hayashi, T. *Chem. Lett.* **1992**, 2177.

(9) Thuilliez, A. DEA University Paris VI, June 1998.

(10) 12.3 ppm in DMSO, see: Wehman, P.; van Donge, H. M. A.; Hagos, A.; Kamer, P. C. J.; van Leeuwen, P. W. N. M. *J. Organomet. Chem.* **1997**, *535*, 183.

(11) For an accelerating effect of water on the kinetics of formation of Pd^0 complexes, see ref 8.

(12) As observed by Kollar et al, a mixture of $Pd(OAc)_2$ and 1 equiv of dppp gave rise to an undefined Pd^0 complex. Reactions were then conducted from mixtures of $Pd(OAc)_2$, 1 equiv of dppp, and 1 or 2 equiv of PPh_3, leading to competition between dppp and PPh_3 for the reduction of the Pd^{II} center. See: Csakai, Z.; Skoda-Földes, R.; Kollar, L. *Inorg. Chim. Acta* **1999**, *286*, 93.

Scheme 4. Mechanism of the Formation of Pd^0 from $Pd(OAc)_2$ and 2 equiv of dppp in DMF

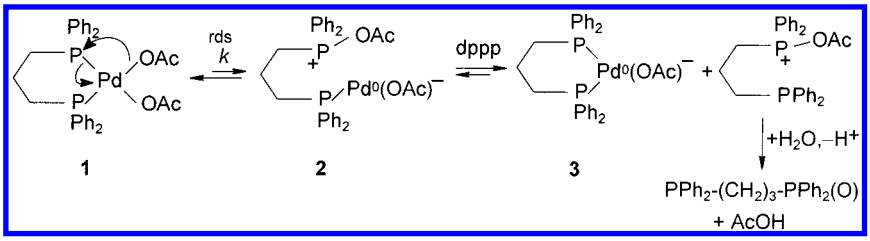

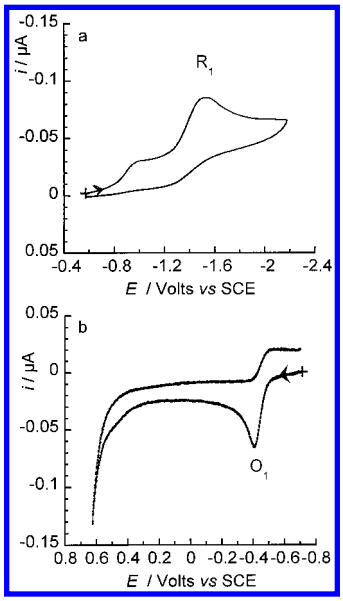

Figure 1. Cyclic voltammetry performed in DMF (containing nBu$_4$NBF$_4$, 0.3 M) at a steady gold disk electrode (0.5 mm diameter in a and 2 mm diameter in b; scan rate 0.2 V s^{-1}) at 20 °C. (a) $Pd(OAc)_2$ (2 mM) and dppp (4 mM): reduction of $Pd(OAc)_2$(dppp). (b) Oxidation of the Pd^0 complex generated from $Pd(OAc)_2$ (2 mM) and dppp (4 mM), 120 s after mixing.

dition of water, indicative of an equilibrated reaction shifted to completion by water (as observed by Osawa and Hayashi in the case of Binap[8]), a phenomenon that was not observed when only 1 equiv of dppp was added to $Pd(OAc)_2$ (vide supra). The stability of the Pd^0 complex was improved in the presence of a base such as NEt_3, as observed for PPh_3.[2] This was interpreted as a stabilization of the anionic complex $Pd^0(PPh_3)_2(OAc)^-$ vis à vis its decomposition to the unstable $Pd^0(PPh_3)_2$ by the protons (formed concomitantly with the Pd^0 complex, Scheme 1) prone to react with the ligated acetate to form acetic acid.[3] By analogy, one deduces that the Pd^0 complex formed from $Pd(OAc)_2$ and 2 equiv of dppp is also an anionic Pd^0 complex ligated by one acetate, which is stabilized in the presence of a base (eq 6). Moreover, in ^{31}P NMR, it appears as a singlet, indicative of two equivalent ^{31}P.

$$Pd^0(dppp)(OAc)^- + H^+ \xrightarrow{NEt_3} Pd^0(dppp) + AcOH \qquad (6)$$

Therefore, a tentative overall reaction can then be expressed as in eq 7, at this preliminary stage in the study.

$$Pd(OAc)_2(dppp) + dppp + H_2O \longrightarrow Pd^0(dppp)(OAc)^- + dppp(O) + AcOH + H^+ \qquad (7)$$

To take into account the important role of the second dppp ligand as well as the noninfluence of water on the rate of formation of a Pd^0 complex in the presence of only 1 equiv of dppp, a mechanism is proposed (Scheme 4), which differs from the tentative mechanism proposed earlier in Scheme 3.

In the presence of an extra dppp, a fast reversible ligand substitution occurs on the Pd^0 complex **2**, formed in the slow intramolecular reduction step (**1** → **2**). The overall reaction goes to completion by hydrolysis of the released phosphonium salt, which produces the hemioxide dppp(O) (Scheme 4).

As performed in earlier works of this group for PPh_3,[1] the rate of formation of the Pd^0 complex from a solution of $Pd(OAc)_2$ (2 mM in DMF containing nBu$_4$NBF$_4$, 0.3 M) and dppp (2 equiv) was monitored by amperometry at a rotating gold disk electrode polarized at −0.1 V, on the oxidation plateau wave of the Pd^0 complex. The oxidation current intensity of the Pd^0 complex (proportional to its concentration) was recorded as a function of time (Figure 2a): (i) at 48 °C to have reasonable reaction times, (ii) in the presence of water (20 equiv) to observe an overall irreversible reaction, and (iii) in the presence of NEt_3 (30 equiv) to avoid the decomposition of the generated Pd^0 complex. The plot of $\ln[(i_{lim} - i)/i_{lim}]$ versus time was linear (Figure 2b), characteristic of a first reaction order in palladium: $(i_{lim} - i)/i_{lim} = ([Pd^0]_{lim} - [Pd^0])/[Pd^0]_{lim}$ with i_{lim} = oxidation current intensity at infinite time and i = oxidation current intensity at t. The rate constant k for the formation of the Pd^0 complex **3** (Scheme 4, where the irreversible reaction **1** → **2** is rate determining) is then determined from the slope of the regression line (Figure 2b). $\ln(([Pd^0]_{lim} - [Pd^0])/[Pd^0]_{lim}) = -kt$ with $k = 2.8 \times 10^{-3}$ s^{-1} at 48 °C. The formation of a Pd^0 complex from $Pd(OAc)_2$ and 2 equiv of dppp is thus slightly slower than that from PPh_3 ($k = 3.6 \times 10^{-3}$ s^{-1} at 48 °C).[1b]

When only 1 equiv of dppp was considered, the reverse reaction **2** → **1** became preponderant so that no Pd^0 complex was formed at room temperature. The reverse reaction **2** → **1** is in fact an *intramolecular* oxidative addition of a phosphonium salt to a Pd^0 center (activation of the P−OAc bond in complex **2**), which was not observed when starting from $Pd(OAc)(PPh_3)_2$[1] because it would then be *intermolecular* (Scheme 1). This explains why the reduction step in the case of PPh_3 was irreversible (Scheme 1) and why no accelerating effect of water was observed.[1]

$Pd(OAc)_2$ + 3 equiv of dppp. Addition of 3 equiv of dppp to $Pd(OAc)_2$ in DMF (containing nBu$_4$NBF$_4$, 0.3 M) together with 30 equiv of NEt_3 and 1 equiv of H_2O results in the formation of a yellow-orange solution, which exhibited the reduction peak of $Pd(OAc)_2$(dppp). When the cyclic voltammetry was performed from time to time, the reduction current intensity decreased up

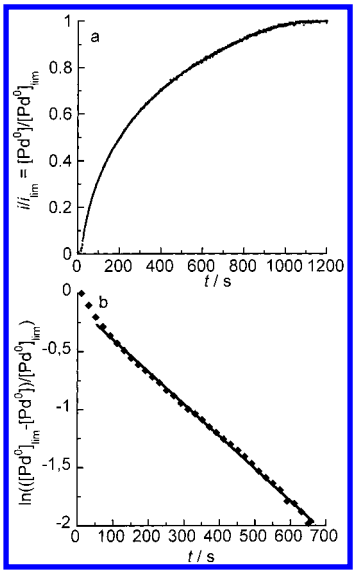

Figure 2. Kinetics of the formation of the Pd^0 complex generated from $Pd(OAc)_2$ (2 mM) and dppp (4 mM), under conditions where the reaction is irreversible, i.e., in the presence of H_2O (40 mM) and NEt_3 (60 mM), monitored as a function of time at a rotating gold disk electrode (2 mm diameter, ω = 105 rad s^{-1}) polarized at −0.1 V. (a) Variation of $i/i_{lim} = [Pd^0]/[Pd^0]_{lim}$ with time (i_{lim} = oxidation current intensity at infinite time, i = oxidation current intensity at t). (b) (◆): experimental variation of $\ln((i_{lim}-i)/i_{lim}) = \ln(([Pd^0]_{lim} - [Pd^0])/[Pd^0]_{lim})$ with time; solid line: $\ln(([Pd^0]_{lim} - [Pd^0])/[Pd^0]_{lim}) = -kt$ with $k = 2.8 \times 10^{-3}$ s^{-1} at 48 °C.

to zero while the oxidation peak of a Pd^0 complex at −0.41 V was observed, its oxidation peak current intensity increasing with time. However, this oxidation peak did not disappear after addition of PhI (30 equiv).

The formation of the Pd^0 complex was monitored by ^{31}P NMR spectroscopy. The magnitude of the singlet of $Pd(OAc)_2(dppp)$ at 11.0 ppm decreased with time, while the singlet of the Pd^0 complex at 4.2 ppm increased with time. dppp(O) was also detected on the spectrum by its two characteristic singlets (vide supra). As observed in cyclic voltammetry, the Pd^0 complex did not react with PhI. This is consistent with the formation of the coordinately saturated 18-electron complex $Pd^0(dppp)_2$ (eqs 8, 9), known to be nonreactive in oxidative additions of aryl halides.[13]

$$Pd(OAc)_2(dppp) + 2dppp + H_2O \rightarrow Pd^0(dppp)_2 + dppp(O) + 2AcOH \quad (8)$$

$$Pd^0(dppp)_2 + PhI \longrightarrow\!\!\!\!\!\times\!\!\!\!\!\rightarrow PhPdI(dppp) + dppp \quad (9)$$

The rate of formation of $Pd^0(dppp)_2$ determined at 48 °C by the amperometry technique (vide supra) was similar to that of the Pd^0 complex generated from $Pd(OAc)_2$ + 2 equiv of dppp. This confirms that the rate-determining step is indeed the reaction **1** → **2** (Scheme 4), followed by the fast ligand exchange by one or two dppp ligands according to the dppp excess.

Complex Formed in the Oxidative Addition of PhI to the Pd^0 Complex Generated in Situ from $Pd(OAc)_2$ and 2 equiv of dppp in DMF. Addition of

Scheme 5. Oxidative Addition of PhI to the Pd^0 Complex Generated from $Pd(OAc)_2$ and 2 equiv dppp in DMF

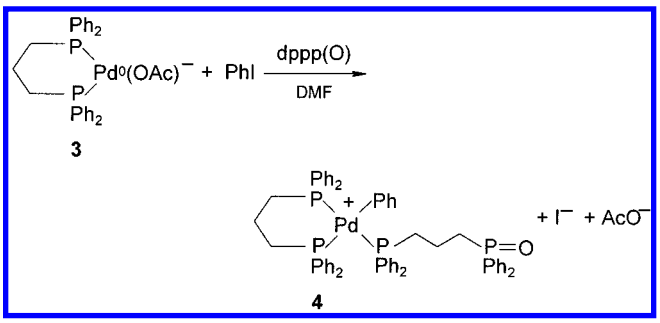

PhI to the Pd^0 complex formed quantitatively in a solution of $Pd(OAc)_2$ with 2 equiv of dppp in the presence of NEt_3 (3 equiv) in DMF gave a (phenyl)palladium(II) complex. The signal of the Pd^0 complex at 4.20 ppm was no longer observed as well as the signal at −17.0 ppm characteristic of the nonoxidized PPh_2 moiety of the hemioxide dppp(O). The ^{31}P NMR spectrum of the (phenyl)palladium(II) complex revealed a complex structure involving three different ^{31}P ligated to the Pd^{II} center: 15.0 ppm (dd $J_{PPtrans}$ = 359 Hz, J_{PPcis} = 34 Hz, PPh_2 of dppp(O) cis to Ph), 7.9 ppm (dd, $J_{PPtrans}$ = 359 Hz, J_{PPcis} = 51 Hz, P of dppp cis to Ph), −3.1 ppm (dd, J_{PPcis} = 34 and 51 Hz, P of dppp trans to Ph). An additional singlet at 29.7 ppm characterizes the P═O moiety of the mono-ligated dppp(O). This gives evidence for a structure of complex **4** (Scheme 5) in which the Pd^{II} is bis-ligated by one dppp and mono-ligated by the hemioxide dppp(O) (formed concomitantly with the Pd^0 complex) acting thus as a monodentate ligand.

The rationalization given above (Scheme 5) requires that the 16-electron four-ligated complex **4**, PhPd(dppp)-(dppp(O))$^+$, is a cationic complex. Its ionic character was confirmed by conductivity measurements. The initial conductivity due to the ionic character of the Pd^0 complex (2 mM in DMF) formed in eq 7 increased from 5.4 to 39 μS after addition of PhI (10 equiv).[14] The presence of released I^- was confirmed by cyclic voltammetry. One oxidation peak was indeed detected at +0.45 V vs SCE and readily assigned to the oxidation of free I^-, by comparison with that of an authentic sample of n-Bu_4NI. The structure of a related complex, p-CN-C_6H_4-Pd(dppp)(dppp(O))$^+$, very similar to complex **4**, has been observed by Hallberg and Larhed,[16] based on electrospray mass spectroscopy during a Heck reaction from p-CN-C_6H_4OTf with $Pd(OAc)_2$/dppp as the catalytic precursor. The value M = 1048 implies the mono-complexation of dppp(O), as evidenced in the present work by different approaches.

In contrast to PPh_3, for which $PhPd(OAc)(PPh_3)_2$ was formed in the oxidative addition of PhI (Scheme 2),[1−3] PhPd(OAc)(dppp) was not formed. It was however produced quantitatively after addition of n-Bu_4NOAc in excess (10 equiv) (eq 10) and identified by its ^{31}P NMR spectrum—two doublets at −3.7 ppm (J_{PP} = 48 Hz) and

(13) (a) Fitton, P.; Rick, E. A. *J. Organomet. Chem.* **1971**, *28*, 287. (b) Amatore, C.; Broeker, G.; Jutand, A.; Khalil, F. *J. Am. Chem. Soc.* **1997**, *119*, 5176.

(14) The conductivity increase is compatible with that observed for cationic arylpalladium(II) complexes.[15]

(15) Jutand, A.; Mosleh, A. *Organometallics* **1995**, *14*, 1810.

(16) Hallberg, A; Larhed, M. Personal communication at the Post-OMCOS-10 Symposium, Paris, July 1999.

19.4 ppm (J_{PP} = 48 Hz)—similar to the one reported in the literature.[17]

$$PhPd(dppp)(dppp(O))^+ + AcO^- \xrightarrow{fast} PhPd(OAc)(dppp) + dppp(O) \quad (10)$$

The addition of nBu$_4$NI in excess (10 equiv) resulted in the formation of PhPdI(dppp) (eq 11), identified by comparison of its ^{31}P NMR spectrum with that of an authentic sample (two doublets at −8.6 ppm (J_{PP} = 53 Hz) and 12.4 ppm (J_{PP} = 53 Hz)).[13b] However this reaction was considerably slower than that of AcO$^-$ ions.

$$PhPd(dppp)(dppp(O))^+ + I^- \xrightarrow{slow} PhPdI(dppp) + dppp(O) \quad (11)$$

Consequently the structure of the (aryl)Pd^{II}(dppp) complex formed in the oxidative addition of a Pd^0 complex generated from Pd(OAc)$_2$/2dppp strongly depends on the aryl derivative considered: (i) four-ligated cationic ArPd(dppp)(dppp(O))$^+$ complexes are formed when starting from aryl triflates;[16] (ii) cationic ArPd(dppp)(dppp(O))$^+$ complexes are formed in the very first catalytic cycles when starting from aryl iodides and then neutral ArPdI(dppp) complexes produced by reaction of I$^-$ released in the catalytic reaction; (iii) ArPd(OAc)(dppp) complexes are formed in the presence of excess acetate ions (often used as a base in Heck reactions)[5] whatever the aryl iodides/triflates derivatives. We must also take into account that all these complexes might be involved in equilibrium, as we previously established for ArPdI(PPh$_3$)$_2$, ArPd(OAc)(PPh$_3$)$_2$, and ArPd(PPh$_3$)$_2^+$.[18] It is worthwhile to note that, in DMF, complexes ligated by three phosphines, ArPd(PPh$_3$)$_3^+$, have never been detected in appreciable amount even in the presence of PPh$_3$ in large excess,[15] whereas ArPd(dppp)(dppp(O))$^+$ complexes are formed due to less steric hindrance of dppp when compared to PPh$_3$.

Rate and Mechanism of the Oxidative Addition of PhI to the Pd^0 Complex Generated in Situ from Pd(OAc)$_2$ and 2 equiv of dppp in DMF. The oxidative addition of PhI to the Pd^0 complex generated in situ from Pd(OAc)$_2$ (2 mM in DMF) and 2 equiv of dppp, in the presence of NEt$_3$ (30 equiv) and H$_2$O (20 equiv), was monitored by amperometry, as performed previously for PPh$_3$.[2] The rotating electrode was polarized at −0.1 V, on the plateau of the oxidation wave of the Pd^0 complex. The decay of the oxidation current intensity, proportional to the Pd^0 concentration, was recorded versus time after addition of PhI (5 equiv) at 48 °C. The solution turned from orange-yellow to pale yellow. From the curve obtained in Figure 3a, one already observes that the decay of the Pd^0 concentration does not obey a classical decreasing exponential curve, fitting with a reaction order of +1 for Pd^0, as reported for Pd^0(PPh$_3$)$_2$(OAc)$^-$,[2] suggesting a more complicated mechanism for the oxidative addition. It is important to note that, under similar conditions, the Pd^0 complex generated from Pd(OAc)$_2$ and 2 equiv of dppp is considerably less reactive with PhI (by a factor 300) than Pd^0(PPh$_3$)$_2$(OAc)$^-$ generated from Pd(OAc)$_2$ and 3 equiv of PPh$_3$.[3]

In a first approach, the influence of ions such as AcO$^-$ or I$^-$, which are released in the oxidative addition (Scheme 5), has been investigated. They could indeed coordinate the Pd^0 and consequently affect its reactivity in the course of the oxidative addition.[2,3,19] No effect of I$^-$ (5 equiv of nBu$_4$NI added before PhI) was observed on the kinetics. However, the kinetics was affected by the presence of AcO$^-$ ions. First of all, the oxidative addition was faster as soon as 1 equiv of nBu$_4$NOAc was added before PhI. Second, the kinetics became well reproducible[20] in the presence of AcO$^-$ with a kinetic curve still not compatible with an exponential decay (Figure 3b). This suggests that AcO$^-$ ions, when in excess, may interfere in the oxidative addition process by changing the structure of the Pd^0 complex initially produced from Pd(OAc)$_2$ and 2 equiv of dppp. When AcO$^-$ ions (10 equiv) were added together with Pd(OAc)$_2$ and 2 equiv of dppp at 48 °C, the rate of formation of the Pd^0 complex was faster but the resulting Pd^0 complex was not so stable (the solution turned progressively to brown) and decomposed slowly within 75 min, after a variable induction period, thus exceeding the duration required for the investigated oxidative additions (20 min). The accelerating effect of AcO$^-$ ions on the rate of formation of the Pd^0 complex may be regarded as featuring an irreversible trapping of the intermediate complex **2** as complex **5** (eq 12), this reaction being faster than the reactions **2** → **1** or **2** → **3** in Scheme 4. At this level, we do not know whether the observed Pd^0 decomposition is that of complex **5** or of a further complex.

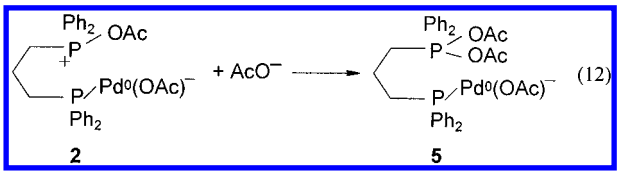

(12)

When the AcO$^-$ ions were added once the Pd^0 complex has been formed quantitatively from Pd(OAc)$_2$ + 2 equiv dppp, the decomposition time of the resulting Pd^0 was considerably longer than the time required for the oxidative addition. This latter procedure was therefore adopted for the detailed mechanistic investigation of the oxidative addition. PhI was added just after addition of AcO$^-$ ions. The final complex formed in the oxidative addition was then PhPd(OAc)(dppp).

The kinetics of the oxidative addition of PhI (5 equiv) has been investigated as a function of the AcO$^-$ concentration in the range 1−15 equiv. Figure 4 exhibits the plot of $1/t_{1/2}$ versus AcO$^-$ concentration ($t_{1/2}$ = half reaction time of the oxidative addition). The reaction is then first order in AcO$^-$ at low AcO$^-$ concentrations, while it becomes zero order at higher AcO$^-$ concentrations (over 7 equiv of AcO$^-$). The saturating effect suggests that AcO$^-$ ions are involved in an equilibrium, which delivers the reactive Pd^0 complex and which is completely shifted toward this reactive species as soon as 7 equiv of AcO$^-$ are present.

Whatever the AcO$^-$ concentration, at low PhI concentrations (less than 10 equiv) the reaction order in Pd^0 is neither 1 nor 0 but 1/2, as shown by the linear

(17) Ludwig, M.; Strömberg, S.; Swensson, B.; Akermark, B. *Organometallics* **1999**, *18*, 970.
(18) Amatore, C.; Carré, E.; Jutand, A. *Acta Chem. Scand.* **1998**, *52*, 100.
(19) Amatore, C.; Azzabi, M.; Jutand, A. *J. Am. Chem. Soc.* **1991**, *113*, 8375.
(20) The kinetics were not reproducible in the absence of added AcO$^-$, probably because of the formation of aggregates.

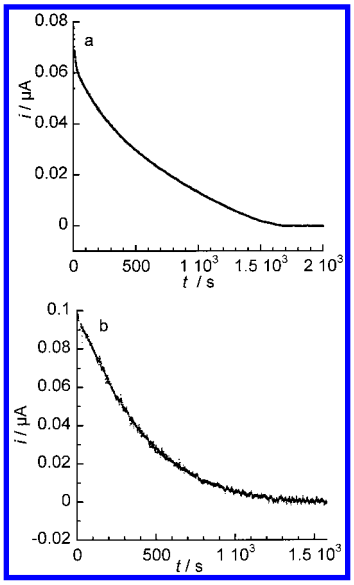

Figure 3. Kinetics of the oxidative addition of PhI to the Pd^0 complex generated from $Pd(OAc)_2$ (2 mM) and dppp (4 mM) in the presence of H_2O (40 mM) and NEt_3 (60 mM), monitored as a function of time at a rotating gold disk electrode (2 mm diameter, $\omega = 105$ rad s^{-1}) polarized at −0.1 V. 48 °C. (a) Variation of the oxidation current intensity i (proportional to the Pd^0 concentration) with time in the presence of PhI (10 mM). (b) Same reaction in the presence of nBu$_4$NOAc (30 mM) added to the Pd^0 complex before PhI.

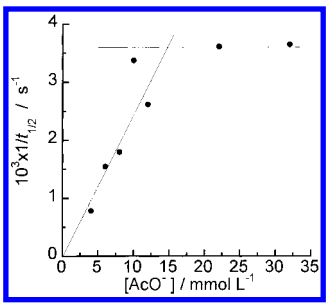

Figure 4. Kinetics of the oxidative addition of PhI to the Pd^0 complex generated from $Pd(OAc)_2$ (2 mM) and dppp (4 mM) in the presence of H_2O (40 mM) and NEt_3 (60 mM) monitored as a in Figure 3, at 48 °C. The kinetics is investigated in the presence of various amounts of AcO^- ions added as nBu$_4$NOAc just before PhI (10 mM). Plot of $1/t_{1/2}$ ($t_{1/2}$ = half reaction time) vs AcO^- concentration (total concentration including the acetate released from AcOH when the reaction 7 is performed in the presence of NEt_3).

plot of $(i/i_0)^{1/2} = ([Pd^0][Pd^0]_0)^{1/2}$ versus time (Figure 5a) (i = oxidation current intensity of Pd^0 at t; i_0 = initial oxidation current intensity of Pd^0), in agreement with the kinetic law given in eq 13.

$$d[Pd^0]/dt = -k_{obs}[Pd^0]^{1/2} \qquad ([Pd^0]/[Pd^0]_0)^{1/2} = -k_{obs}t/2[Pd^0]_0^{1/2} + 1 = (i/i_0)^{1/2} \quad (13)$$

k_{obs} is then calculated from the slope (Figure 5a): $k_{obs} = 8.6 \times 10^{-5}$ $M^{1/2}$ s^{-1} (vide infra).

At higher PhI concentrations (over 10 equiv) and whatever the AcO^- concentration, we observed a deviation from the reaction order of 1/2 (Figure 5b) at longer reaction times. This is consistent with the superposition

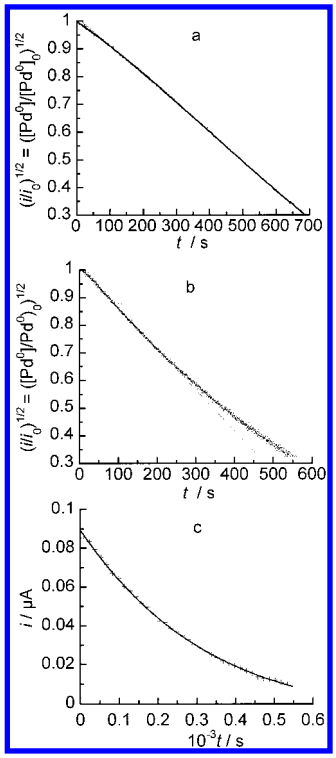

Figure 5. Kinetics of the oxidative addition of PhI to the Pd^0 complex generated from $Pd(OAc)_2$ (2 mM) and dppp (4 mM) in the presence of H_2O (40 mM) and NEt_3 (60 mM) monitored at a rotating disk electrode, as a in Figure 3b, at 48 °C. (a) nBu$_4$NOAc (8 mM), PhI (10 mM); plot of $(i/i_0)^{1/2} = ([Pd^0][Pd^0]_0)^{1/2}$ vs time (i = oxidation current intensity of Pd^0 at t; i_0 = initial oxidation current intensity of Pd^0). (b) nBu$_4$NOAc (30 mM), PhI (160 mM); plot of $(i/i_0)^{1/2} = ([Pd^0][Pd^0]_0)^{1/2}$ vs time. (c) nBu$_4$NOAc (30 mM), PhI (160 mM); (+): plot of i (i = oxidation current intensity of Pd^0 at t) vs time. The solid line is the simulated theoretical curve using the kinetic law: $i = (i_0/C_0)\{(C_0 1/2 + k_{obs}/k'_{obs})\text{-}e^{-k'_{obs}\times t/2} - k_{obs}/k'_{obs}\}^2$ with $k_{obs} = 5.3 \times 10^{-5}$ $M^{1/2}$ s^{-1}, $k'_{obs} = 2.1 \times 10^{-3}$ s^{-1}, and $C_o = 2$ mM.

of a second kinetics with a reaction order of +1 for Pd^0, as established by comparison with a theoretical kinetic curve (Figure 5c, [PhI] = 160 mM, $[Pd^0]_0 = C_0 = 2$ mM) simulated using the kinetic law of eq 14c, with $k_{obs} = 5.3 \times 10^{-5}$ $M^{1/2}$ s^{-1} and $k'_{obs} = 2.1 \times 10^{-3}$ s^{-1}.

$$d[Pd^0]/dt = -k'_{obs}[Pd^0] - k_{obs}[Pd^0]^{1/2} \quad (14a)$$

$$[Pd^0] = \{([Pd^0]_0 1/2 + k_{obs}/k'_{obs})e^{-k'_{obs}\times t/2} - k_{obs}/k'_{obs}\}^2 \quad (14b)$$

$$i = (i_0/C_0)\{(C_0^{1/2} + k_{obs}/k'_{obs})e^{-k'_{obs}\times t/2} - k_{obs}/k'_{obs}\}^2 \quad (14c)$$

According to this hypothesis, the oxidative addition proceeds by two parallel pathways, one with a reaction order of +1/2 in Pd^0, the second one involving a reaction order of +1 in Pd^0 showing up mostly at high PhI concentrations. This dual mechanism is operating whatever the AcO^- concentration. The reaction order in PhI was determined at high AcO^- concentrations (>7 equiv) when the kinetics did not depend on the AcO^- concentrations. The plots of k_{obs} and k'_{obs} versus PhI concentration are reported in Figures 6a,b, respectively. When the reaction order in Pd^0 is 1/2, the reaction order in

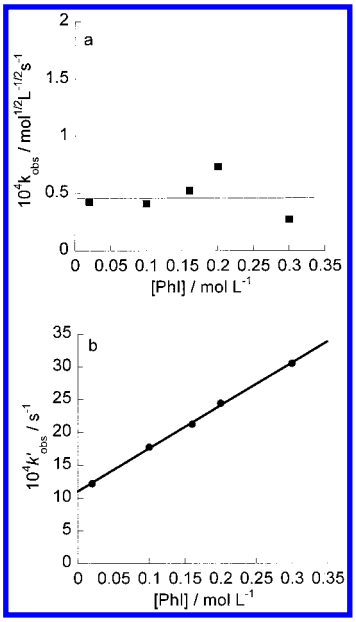

Figure 6. Kinetics of the oxidative addition of PhI (in the range 20−350 mM) to the Pd^0 complex generated from $Pd(OAc)_2$ (2 mM) and dppp (4 mM) in the presence of H_2O (40 mM) and NEt_3 (60 mM) monitored at a rotating disk electrode, as a in Figure 5c, at 48 °C. $v = k'_{obs}[Pd^0] + k_{obs}[Pd^0]^{1/2}$. (a) Variation of k_{obs} vs PhI concentration. (b) Variation of k'_{obs} vs PhI concentration.

Scheme 6. Minimal Mechanism for the Oxidative Addition

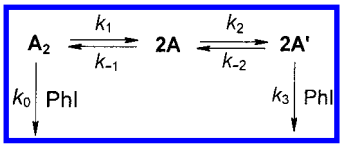

PhI is 0 (k_{obs} is constant, Figure 6a). This means that the rate-determining step of the overall oxidative addition does not involve PhI but is a step in which a reactive monomeric Pd^0 complex is formed from a dimer (order 1/2 in Pd^0). When the reaction order in Pd^0 is +1, the reaction order in PhI is not strictly +1 since the straight line for the variation of k'_{obs} does not intercept at the origin (Figure 6b); thus $k'_{obs} = a[PhI] + b$. On the basis of these experimental results, the simplest mechanism, which rationalizes all findings, is proposed in Scheme 6. A reactive dimeric Pd^0 species $\mathbf{A_2}$ leads to two successive equilibria involving a nonreactive monomeric Pd^0 species **A** and another one **A′**, which reacts with PhI in parallel (Scheme 6).

Indeed, provided that the various rate constants are adequate, this mechanism displays all the experimentally observed features:

• At low PhI concentrations, $k_0[PhI] \ll k_1$ and the monomer **A′** is the only reactive species. The kinetic law for the disappearance of the dimer $\mathbf{A_2}$ is then given by the eq 15a, after considering a fast equilibrium between $\mathbf{A_2}$ and **2A** and the steady-state approximation for **A′**.

$$v = 2k_3[\mathbf{A'}][PhI] = 2k_2k_3[\mathbf{A}][PhI]/(k_{-2} + k_3[PhI]) \quad (15a)$$

When $k_3[PhI] \gg k_{-2}$, one obtains eq 15b.

$$v = 2k_2[\mathbf{A}] = 2k_2(k_1/k_{-1})^{1/2}[\mathbf{A_2}]^{1/2} = k_{obs}[\mathbf{A_2}]^{1/2} \quad (15b)$$

Scheme 7. Mechanism for the Oxidative Addition

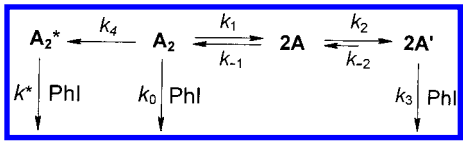

This kinetic law is then in agreement with the experimental reaction order of 1/2 found for Pd^0 and 0 for PhI with $k_{obs} = (5 \pm 1) \times 10^{-5}$ $M^{1/2}$ s^{-1} (Figure 6a), a value compatible with that found above.

$$k_{obs} = 2k_2(k_1/k_{-1})^{1/2}, \text{ then } k_2(k_1/k_{-1})^{1/2} = (2.5 \pm 0.5) \times 10^{-5}\ M^{1/2}\ s^{-1}$$

• At higher PhI concentrations, $k_0[PhI] \gg k_1$ and the oxidative addition proceeds not only from **A′** but also from $\mathbf{A_2}$ in competition with its dissociation (Scheme 6).

The kinetic law is then expressed as in eq 16a.

$$v = k_0[\mathbf{A_2}][PhI] + 2k_3[\mathbf{A'}][PhI] = k_0[\mathbf{A_2}][PhI] + 2k_2k_3[\mathbf{A}][PhI]/(k_{-2} + k_3[PhI]) \quad (16a)$$

With the same hypothesis as above: $k_3[PhI] \gg k_{-2}$, one gets eq 16b.

$$v = k_0[\mathbf{A_2}][PhI] + 2k_2(k_1/k_{-1})^{1/2}[\mathbf{A_2}]^{1/2} \quad (16b)$$

The kinetic law (eq 16b) is in agreement with the experimental reaction order of 1/2 for Pd^0 and 0 for PhI found above in addition to an experimental reaction order of 1 found for Pd^0. However, in the latter case, the reaction order is strictly 1 in PhI, which was not observed experimentally (see the variation of k'_{obs} in Figure 6b). This implies that the dimer $\mathbf{A_2}$ should also disappear along a concurrent path being zero order in PhI. This may arise to give an inactive or active dimeric complex $\mathbf{A_2}$* (Scheme 7).

The corresponding kinetic law is then given in eq 17.

$$v = k_0[\mathbf{A_2}][PhI] + k_4[\mathbf{A_2}] + 2k_2(k_1/k_{-1})^{1/2}[\mathbf{A_2}]^{1/2} = k'_{obs}[\mathbf{A_2}] + k_{obs}[\mathbf{A_2}]^{1/2} \quad (17)$$

$$k'_{obs} = k_0[PhI] + k_4 = a[PhI] + b \quad \text{(see eq 14a and Figure 6b)}$$

From Figure 6b one deduces $k_0 = 6.5 \times 10^{-3}$ M^{-1} s^{-1} and $k_4 = 1.1 \times 10^{-3}$ s^{-1}.

The saturating effect of acetate ions on the kinetics of the oxidative addition, observed at high AcO^- and low PhI concentrations (Figure 4), implies that the AcO^- ions are involved in an equilibrium, which produces the Pd^0 dimer $\mathbf{A_2}$ with a reaction order of +1 for AcO^- (Figure 4). This equilibrium would be completely shifted toward the dimer $\mathbf{A_2}$ as soon as 7 equiv of AcO^- are added to the solution, in which a Pd^0 complex has been formed spontaneously from $Pd(OAc)_2$ and 2 equiv of dppp. The complex $\mathbf{A_2}$ is then the major Pd^0 species. This suggests that the Pd^0 complex, formed from $Pd(OAc)_2$ and 2 equiv of dppp, is not $Pd^0(dppp)(OAc)^-$ (**3**) as tentatively proposed in Scheme 4, but probably a dimer $\mathbf{A_2^0}$ formed from $Pd^0(dppp)(OAc)^-$, due to the bidentate character of dppp (Scheme 8). The dimer $\mathbf{A_2^0}$,

Scheme 8. Mechanism for the Oxidative Addition of PhI to the Pd^0 Complex Generated from $Pd(OAc)_2$ and 2 equiv of dppp in the Presence of AcO^- Ions[a]

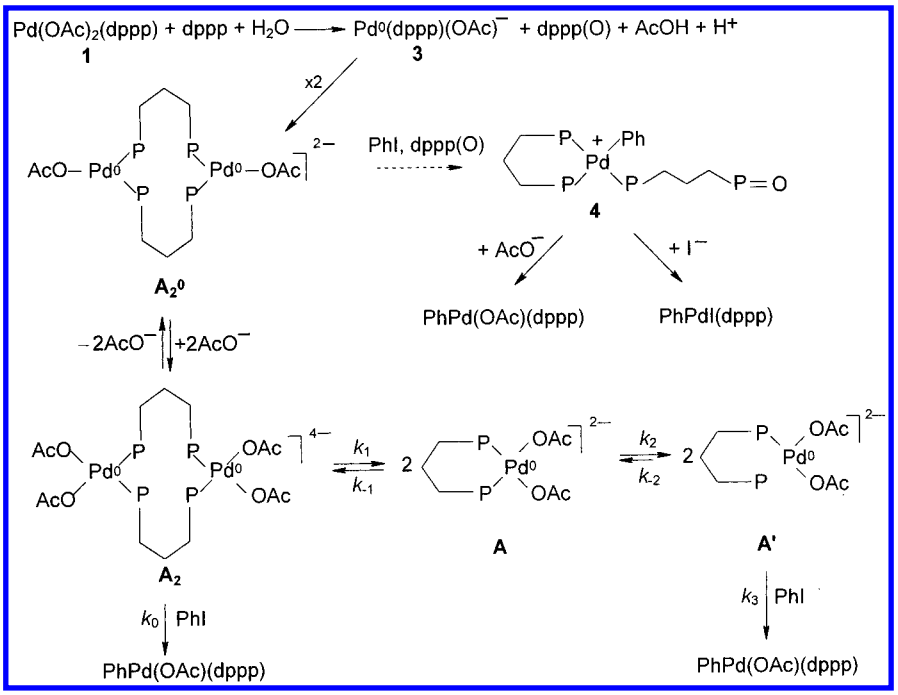

[a]For more clarity, the two Ph ligands of the P atoms have been omitted.

with two 16-electron Pd^0 centers, can be coordinated to extra AcO^- to form a new Pd^0 dimer, $\mathbf{A_2}$. This dissociates into a nonreactive 18-electron complex **A**. The cleavage of the a P−Pd bond is then required to produce a reactive 16-electron Pd^0 complex, **A′** (Scheme 8). At high PhI concentration, the dimer $\mathbf{A_2}$ is found to be reactive, although each Pd^0 center has 18 electrons. It probably reacts after an equilibrated cleavage of one P−Pd bond without any modification of the kinetic law. k_0 would then be the apparent rate constant of the overall reaction, i.e. fast equilibrated cleavage of one P−Pd bond (equilibrium constant K_0) followed by a slow oxidative addition of PhI (rate constant k'_0) with $k_0 = K_0 k'_0$.

We are conscious that none of the proposed structures for complex **3**, $\mathbf{A_2^0}$, and $\mathbf{A_2}$ could be characterized. We only know the ^{31}P NMR shift of the Pd^0 complex formed from $Pd(OAc)_2$/2dppp in the absence of extra AcO^- at 4.2 ppm, which is assigned to complex $\mathbf{A_2^0}$. However, the proposed structures for complexes $\mathbf{A_2}$, **A**, and **A′** are consistent with the experimental kinetic results and kinetic laws. So we use them here only as a chemical rationale of the complex mechanistic sequence, which has been fully characterized kinetically (Scheme 7). We do not propose any structure for $\mathbf{A_2^*}$, although there might be an identity between $\mathbf{A_2^*}$ and $\mathbf{A_2^0}$.

Conclusion

As for monodentate phosphine, a Pd^0 complex is spontaneously formed from $Pd(OAc)_2$ and a bidentate phosphine such as dppp. dppp is the reducing agent and is oxidized to the hemioxide dppp(O). In contrast to PPh_3, the intramolecular reduction step is reversible. Consequently, a stable Pd^0 complex is quantitatively formed in the presence of 2 equiv of dppp, water, and a base (NEt_3), which stabilized the Pd^0 complex vis à vis its decomposition by protons, generated by the hydrolysis of a phosphonium salt (Scheme 4). In the presence of 3 equiv of dppp, a nonreactive $Pd^0(dppp)_2$ complex is generated. The oxidative addition with PhI gives a cationic complex $PhPd(dppp)(dppp(O))^+$ (in which dppp(O) behaves as a monodentate ligand) or PhPd(OAc)(dppp) in the presence of added AcO^-. The oxidative addition of PhI is an intricate reaction whose kinetics could be fully investigated only in the presence of added AcO^-. Its involves reactive dimeric or/and monomeric Pd^0 complexes ligated by AcO^-, whose respective reactivity is a function of the PhI concentration (Scheme 8). The complexity of the oxidative addition pathways when performed with a dppp ligand compared to that with a PPh_3 ligand stems from the bidentate character of the dppp ligand which favors dimeric structures.

Experimental Section

General Remarks. ^{31}P NMR spectra were recorded on a Bruker spectrometer (101 MHz) in DMF containing 10% of acetone d_6. Cyclic voltammetry was performed with a homemade potentiostat and a waveform generator Tacussel GSTP4. The cyclic voltammograms were recorded on a Nicolet 301 oscilloscope. Conductivities were measured on a Tacussel CDM210 conductimeter (cell constant = 1 cm^{-1}).

Chemicals. DMF was distilled from calcium hydride under vacuum and kept under argon. $Pd(OAc)_2$, dppp, PhI, nBu$_4$NI, and nBu$_4$NOAc were commercial.

Electrochemical Setup and Electrochemical Procedure for Voltammetry. Experiments were carried out in a three-electrode thermostated cell connected to a Schlenk line. The counter electrode was a platinum wire of ca. 1 cm^2 apparent surface area. The reference was a saturated calomel electrode (Tacussel) separated from the solution by a bridge filled with 3 mL of DMF containing nBu$_4$NBF$_4$ (0.3 M). DMF (12 mL) containing nBu$_4$NBF$_4$ (0.3 M) was introduced into the

cell followed by 5.4 mg (0.024 mmol) of $Pd(OAc)_2$ and then 1−3 equiv of dppp. Cyclic voltammetry was performed at a steady gold disk electrode (0.5 mm or 2 mm diameter) at a scan rate of 0.2 V s^{-1}. Kinetic measurements for the Pd^0 formation and its reactivity with PhI were performed at a rotating gold disk electrode (2 mm diameter, $\omega = 105$ rad s^{-1}) polarized at −0.1 vs SCE.

Acknowledgment. This work has been supported in part by the Centre National de la Recherche Scientifique (CNRS, UMR 8640) and the Ministère de la Recherche (Ecole Normale Supérieure).

OM0101137